Glenoid Rim Anatomy

Risk for Glenoid Vault Perforation During Labral Repair

Yadin D. Levy,* MD, Michael Williamson,† MD, Cesar Flores-Hernandez,‡ BS, Darryl D. D'Lima,‡§ MD, PhD, and Heinz R. Hoenecke Jr,‡ MD

Investigation performed at Shiley Center for Orthopaedic Research and Education at Scripps Clinic, La Jolla, California, USA

Background: Injuries to the glenoid labrum frequently require repair with anchors. Placing anchor devices arthroscopically can be challenging, and anchor malpositioning can complicate surgical outcomes.

Purpose: To determine the safe insertion range and optimal insertion angle of glenoid labral anchors at various positions on the glenoid rim and to establish surgical guidelines that minimize risk of anchor perforation.

Study Design: Descriptive laboratory study.

Methods: Three-dimensional computed tomography scans of 30 normal cadaveric specimens were obtained. A virtual model of a generic labral anchor was inserted into the rim of the glenoid at the clockface positions represented by 12:00, 1:30, 3:00, 4:30, 6:00, 7:30, 9:00, and 10:30. At each position, the safe insertion range was the maximal range measured, and the optimal insertion angle was identified as the angle between the bisector of the safe insertion range and the glenoid face.

Results: Progressing in the clockwise direction, beginning at the 12:00 position, the safe insertion ranges (mean ± SD) were 55.9° ± 10.6°, 63.6° ± 17.6°, 47.7° ± 9.1°, 46.1° ± 8°, 73.9° ± 9.7°, 40.9° ± 6.5°, 40.4° ± 7.4°, and 39.9° ± 7.1°, respectively. The optimal insertion angles were 47.9° ± 7.6°, 53.1° ± 10.9°, 35.0° ± 4.4°, 42.4° ± 4.9°, 60.9° ± 8.4°, 36.6° ± 5.9°, 31.2° ± 4.9°, 34.8° ± 4.6°, respectively.

Conclusion: Optimal insertion angles and safe insertion ranges varied significantly with respect to the position on the glenoid face. The safe insertion range and optimal insertion angle were found to be wider at the anterior glenoid as compared with the posterior glenoid. A posterolateral insertion angle was safer than an anterior insertion angle at the 10:30 position.

Clinical Relevance: Proper arthroscopic technique resulting in anchor insertion at the correct angle, depth, and location will prevent anchor-related glenohumeral complications such as glenoid perforation, cartilage damage, persistent pain, decreased range of motion, and failure of the reconstruction.

Keywords: glenoid labrum; labral tear; labral repair; anchor; shoulder arthroscopy; computer model; virtual surgery

Injuries to the glenoid labrum are common in young athletic patients and can lead to shoulder pain and instability. Primary repair of glenoid labral tears is more widely performed by arthroscopic reattachment of the detached labrum to the glenoid rim with labral anchor devices.[16] While anchors have a large variety in composition, size, and suture configuration, they all utilize the glenoid rim as port of entry into the glenoid vault and the glenoid bone stock as a base for stable attachment. Arthroscopic placement of anchor devices can be challenging because of limited surgical exposure.

Understanding the bony morphology of the glenoid and proper arthroscopic placement of the suture anchor are essential to the success of glenoid labral repairs.[15] An incorrect angle of insertion can lead to perforation of the glenoid vault or damage to the articular cartilage of the glenoid face, resulting in chronic pain, restriction of motion, recurrence of primary pathology, and reoperation.[12] Recent arthroscopic cadaveric studies have shown that the glenoid perforation rate can be as high as 100% during Bankart repair[10] and superior labrum anterior to posterior (SLAP) lesion repair.[6,13] Medial glenoid cortex perforation during SLAP repair increases the risk of suprascapular nerve injury.[6,13,20]

§Address correspondence to Darryl D. D'Lima, MD, PhD, Shiley Center for Orthopaedic Research & Education at Scripps Clinic, 11025 North Torrey Pines Road, Suite 200, La Jolla, CA 92037, USA (e-mail: ddlima@scripps.edu).

*Shiley Center for Orthopaedic Research and Education at Scripps Clinic, La Jolla, California, USA.

†St Luke's Northland Hospital, Kansas City, Missouri, USA.

‡Division of Orthopaedic Surgery, Scripps Clinic, La Jolla, California, USA.

The authors declared that they have no conflicts of interest in the authorship and publication of this contribution.

The Orthopaedic Journal of Sports Medicine, 2(11), 2325967114556257
DOI: 10.1177/2325967114556257
© The Author(s) 2014

This open-access article is published and distributed under the Creative Commons Attribution - NonCommercial - No Derivatives License (http://creativecommons.org/licenses/by-nc-nd/3.0/), which permits the noncommercial use, distribution, and reproduction of the article in any medium, provided the original author and source are credited. You may not alter, transform, or build upon this article without the permission of the Author(s). For reprints and permission queries, please visit SAGE's Web site at http://www.sagepub.com/journalsPermissions.nav.

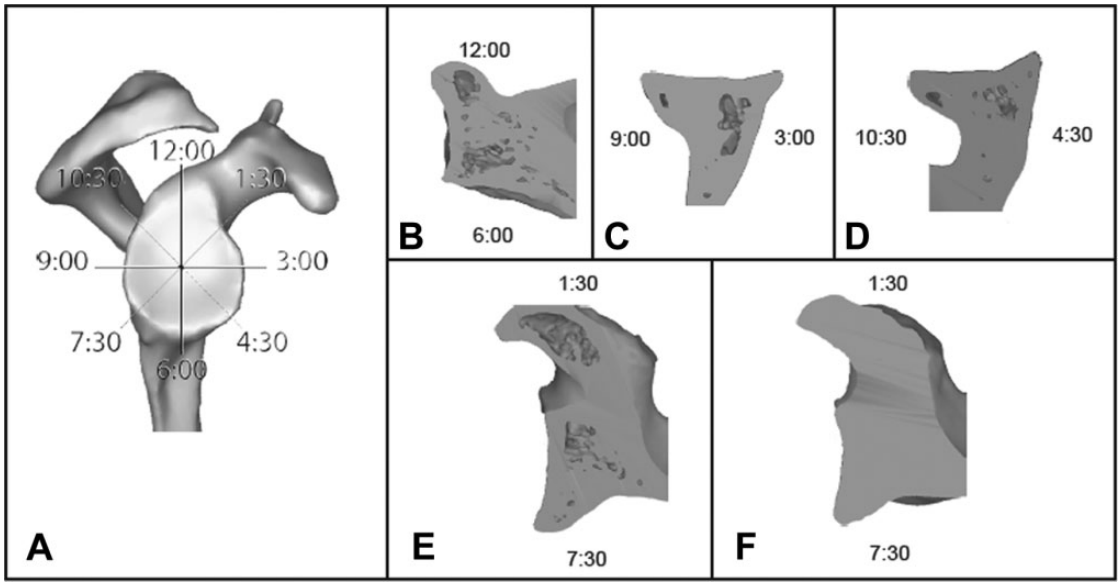

Figure 1. (A) Schematic illustration of the glenoid clockface positions: 12:00, superior position; 3:00, anterior position; 6:00, inferior position; 9:00, posterior position. The lines represent the location of the simulated glenoid cuts and anchor insertion sites. (B) Cross section from 12:00 to 6:00. Note the superior protrusion of the glenoid rim at 12:00 and the continuation with the neck at 6:00. (C) Cross section from 3:00 to 9:00. Note the shelf-like protrusion of the glenoid rim from the glenoid neck at 9:00 and the linear continuation of the rim with the neck at 3:00. (D) Cross section from 4:30 to 10:30. The glenoid bony morphology resembles the cross section morphology of the 3:00 to 9:00 position; however, a slight increase in glenoid rim protrusion was noted at the 10:30 position. (E, F) Cross section at the 1:30 position demonstrated 2 variations: (E) a step-like appearance of the glenoid coracoid junction and (F) a continuous appearance of the glenoid coracoid junction.

Because of scapular anatomy, approaching the posterior glenoid can be clinically challenging. Chan et al[2] demonstrated a high perforation rate during SLAP repair. Their cadaveric study showed 14% perforation rate using a low posterosuperior drill hole utilizing the port of Wilmington at the 10:00 clockface position, and 67% of the perforated glenoids demonstrated suprascapular nerve injury. Lehtinen et al[9] reported glenoid rim angles at 5 anchor locations, corresponding to the 3:00, 4:30, 6:00, 7:30, and 9:00 clockface positions. We also determined the safe insertion range and optimal insertion angle at the 10:30 position (where the acromion complicates the surgical approach) by simulating the use of the Nevaiser portal and posterolateral to the acromion by simulating the use of the portal of Wilmington.

In spite of the reported high glenoid perforation rates and in light of the biomechanical advantage of orthogonal anchor placement relative to the glenoid rim, there are no universally accepted recommendations for surgically safe and optimal insertion angles. The purposes of this study were to (1) determine the safe insertion range available to avoid perforation, (2) determine the optimal insertion angle at various positions on the glenoid rim, and (3) provide surgical guidelines to minimize risk of perforation.

MATERIALS AND METHODS

We performed a high-resolution computed tomography scan (0.625-mm axial resolution) of cadaveric shoulders. After 3-dimensional (3D) reconstruction of the scapulae (in MIMICS; Materialise), an evaluation of the glenoid face was performed, and specimens with any abnormality such as dysplasia, fracture, and bone loss due to arthritic changes were excluded. A total of 30 unpaired normal scapulae (16 left, 14 right) were selected for this study. A glenoid face was oriented to that of a clock, with 12:00 denoting the superior position, 3:00 the anterior position, 6:00 the inferior position, and 9:00 the posterior position. A vertical line was drawn on the glenoid face from 12:00 to 6:00 to measure the height of the glenoid. A perpendicular line to the midpoint of the vertical line was generated from 9:00 to 3:00, passing through the center of the glenoid width to define the center of the glenoid. From the center of the glenoid, a 45° angle was generated to define the 1:30, 4:30, 7:30, and 10:30 positions on the glenoid clockface (Figure 1A).

Measurements of Insertion Angle

A virtual 3 mm–diameter, 15 mm–long model of a generic labral anchor was constructed using a commercially available 3D modeling program (RHINOCEROS 3D; McNeel). The glenoid was radially sectioned with planes that intersected at the glenoid center and that were normal to the glenoid face plane. There were planes that contained the following clockface positions: 1:30, 3:00, 4:30, 6:00, 7:30, 9:00, 10:30, and 12:00. To simplify the analysis, the left-sided scapulae were converted, by mirroring, into

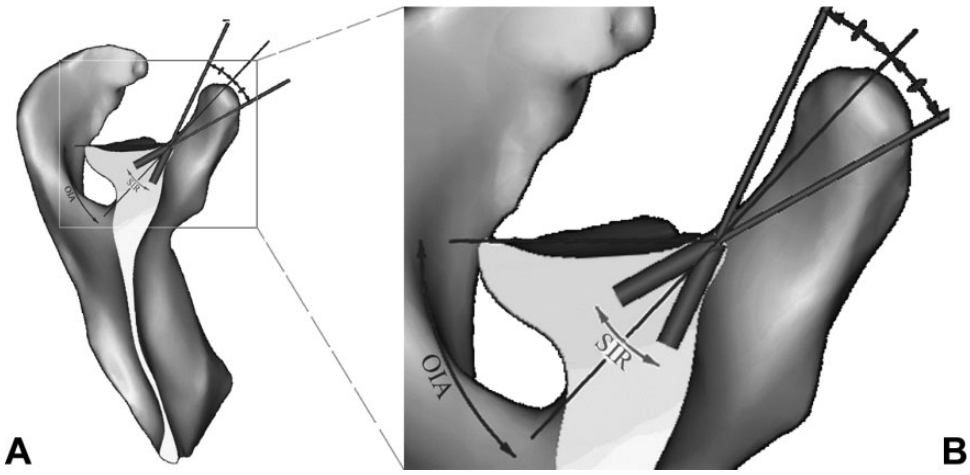

Figure 2. Schematic illustration of a glenoid cross section, anchor placement, and angle measurements: (A) macroscopic appearance, (B) magnified image. The illustration demonstrates the safe insertion range (SIR) and the angle between 2 anchors (one bound by the glenoid articular surface and the other bound by the cortex of the glenoid neck), which represents the maximal measured range. The optimal insertion angle (OIA) is the angle between the bisector of the safe insertion range and the glenoid face. This angle represents the angle with the highest margin for error available for insertion without perforation.

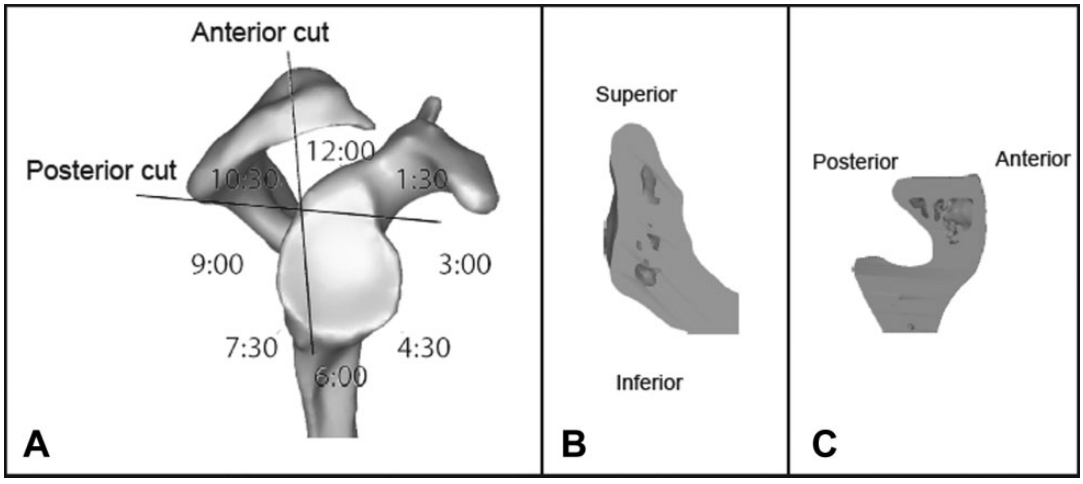

Figure 3. (A) Schematic illustration of the oblique cuts performed at the 10:30 clockface position simulating the use of the Nevaiser portal (anterior to the acromion, anterior cut) and the port of Wilmington (posterolateral to the acromion, posterior cut). (B) The cross-sectional bony morphology after performing the anterior cut, and (C) the posterior cut. Note the difference in the cross-sectional area, which permits a higher insertion range via the port of Wilmington.

right-sided scapulae; therefore, throughout this article when we discuss the clockface position, we refer to 9:00 as posterior and 3:00 as anterior. Figure 1A represents the cross sections in a right scapula. This approach is consistent with previous reports on the glenoid clockface position both in the orthopaedic and the radiologic literature.[3,4,18,19] On each glenoid cross section, 2 anchors were superimposed having a common entry point on the rim of the glenoid: one bounded by the glenoid articular surface and the other bounded by the cortex of the glenoid neck. These 2 positions represented the extreme angles in which the anchor could be placed without perforating through the bone. We defined the "safe insertion range" as the angle between these 2 anchors. This angle represented the widest insertion margin for error available before perforating the glenoid vault. The "optimal insertion angle" was defined by the angle between the bisector of the safe insertion range and the glenoid face (Figure 2). We used the glenoid face as a convenient reference because it was usually well visualized during arthroscopic labral repair.

To simulate avoiding the acromion at the 10:30 position, we performed 2 oblique cuts passing through the 10:30 position on the glenoid rim but not through the center of the glenoid (Figure 3). The safe insertion range and optimal insertion angle at 10:30 were determined anterior to the acromion by simulating the use of the Nevaiser portal

TABLE 1
Optimal Insertion Angle and Corresponding Safe Insertion Range[a]

Anchor Position	Optimal Insertion Angle, deg	Safe Insertion Range, deg
12:00	47.9 ± 7.6	55.9 ± 10.6
1:30	53.1 ± 10.9	63.6 ± 17.6
3:00	35.0 ± 4.4	47.7 ± 9.1
4:30	42.4 ± 4.9	46.1 ± 8.0
6:00	60.9 ± 8.4	73.9 ± 9.7
7:30	36.6 ± 5.9	40.9 ± 6.5
9:00	31.2 ± 4.9	40.4 ± 7.4
10:30	34.8 ± 4.6	39.9 ± 7.1
10:30 (anterior)	17.1 ± 4.1	17.8 ± 4.8
10:30 (posterior)	32.1 ± 3.9	51.3 ± 6.1

[a]Values are reported as mean ± SD.

and posterolateral to the acromion by simulating the use of the portal of Wilmington. At the 6:00 position, we approached the glenoid from superior and inferior to the equator line (the axial plane passing through the 6:00 position) and with angulation of the anchor from anterior to posterior. After each anchor placement was performed, the entire scapula 3D surface was examined to confirm there was no anchor perforation. Two independent readers performed the measurements. The interobserver class coefficient (ICC) was 0.95.

Statistical Analysis

A paired Student *t* test was performed to evaluate statistical differences between the mean safe insertion range and optimal insertion angle at the anterior and posterior clockface positions and between the mean safe insertion range and optimal insertion angle at the anterior and the posterolateral position at the 10:30 clockface position.

RESULTS

Mean morphometric measurements of glenoid length and width were 35.2 ± 2.7 mm and 26.0 ± 2.1 mm, respectively. The cross section of the glenoid at the 3:00 (anteriorly) and 9:00 (posteriorly) positions revealed the typical shelf-like protrusion of the glenoid rim from the glenoid neck at the 9:00, while at the 3:00 position, the glenoid rim did not protrude and blended with the glenoid neck (see Figure 1C).

The mean safe insertion range and the optimal insertion angle are presented in Table 1. The safe insertion range and the optimal insertion angle were significantly wider in the anterior glenoid compared with the posterior glenoid. We chose a difference of 5° or greater as the minimum threshold for intraoperative relevance. On average, the safe insertion angles were greater at anterior insertion sites (1:30, 3:00, and 4:30 positions) compared with their corresponding posterior sites (10:30, 9:00, and 7:30 positions; $P < .001$). The optimal insertion angles were also steeper at anterior insertion sites than their corresponding posterior sites. This result indicates that posterior anchors needed to be inserted more parallel to the glenoid face and had a smaller margin of safety.

At the 10:30 position (superior/posterior), the acromion prevented a direct approach. The optimal insertion angle and the safe insertion range were significantly greater (by 15° and 34°, respectively, $P < .001$) for the posterolateral approach compared with the anterior approach. At the 6:00 position (inferior), approaching the glenoid superior to the equator line would always perforate the glenoid, while approaching the glenoid inferiorly to the equator line with anterior or posterior angulation of the anchor provided a safer insertion range averaging 56°.

No significant difference was observed between the right and left scapulae in the positions studied ($P > .05$).

DISCUSSION

Improper positioning of the suture anchor can lead to glenoid perforation, cartilage damage, persistent pain, damage to suprascapular nerve, decreased range of motion, and failure of the reconstruction, resulting in the need for revision surgery.[5,6,12,17] However, limited data have been published evaluating the anatomy of the glenoid rim.[8,9] Proper arthroscopic technique resulting in anchor insertion at the correct angle, depth, and location may prevent anchor perforation-related glenohumeral complications. Computer navigation systems have been studied in an attempt to increase the accuracy of placing glenoid anchors. The maximum deviation from the target angle was 11.9° during freehand anchor placement and 8.4° during computer-navigated anchor placement.[7] These findings indicate that knowledge of the optimum angle that maximizes the margin of error is very relevant.

In our study, the safe insertion range and optimal insertion angle for placing the labral anchor devices varied significantly with position on the glenoid clockface. We found that anchor insertion in the posterior glenoid rim typically required lower insertion angles (and a smaller safe range) than did insertion in the anterior glenoid (1:30 vs 10:30, 3:00 vs 9:00, 4:30 vs 7:30 positions). This result was a reflection of the difference in the anatomic cross sections around the glenoid clockface (see Figure 1). The protrusion of the posterior glenoid rim from the glenoid neck, especially at the 9:00 position, dictated insertion of the anchor relatively parallel to the glenoid face since insertion of an anchor at steeper angles tended to perforate at the 9:00 position. Lehtinen et al[9] investigated the anteroinferior, inferior, and posterior-inferior glenoid rim anatomy of 20 scapulae computed tomography scans. On average, the glenoid rim angles were greater at the 3:00 (53° ± 5°) than the 9:00 position (49° ± 4°) and lower at the 4:30 (45° ± 7°) than the 7:30 position (61° ± 10°). The trend of these results was partially consistent with our findings. Our study demonstrated a similar trend for the 3:00 and 9:00 positions and an opposite trend for the 4:30 and the 7:30 positions. Moreover, our measured safe insertion ranges were almost similar along the posterior rim that

measured 40.9° ± 6.5°, 40.4° ± 7.4°, and 39.9° ± 7.1° at the 7:30, 9:00, and 10:30 positions, respectively. This finding was of clinical significance as it can increase the surgeons' awareness to the continuous uniformity of the narrow posterior rim and its difference from the anterior rim. In addition, it is important to note that Lehtinen et al[9] determined the optimal angles for insertion by using a line rather than by a virtual anchor. The line did not have a defined width, and the length was variable determined by the distance to the medial cortex of the scapular neck. The authors noted this limitation of their study, stating that if a fixation device was used that was shorter than the distance to the medial cortex, then the arc available for insertion would be different. In our study, we chose an anchor of a common dimension to address this limitation; hence, the magnitudes of our safe insertion ranges were smaller as the use of 3D virtual anchors reduced the safe insertion range within the glenoid rim angle.

At the 1:30 position, we observed a large variation in the relationship between the cross-sectional anatomy of the glenoid and the coracoid process. In some specimens, the base of the coracoid process was wider and continued on to the glenoid rim, which increased the available bone stock and increased the safe insertion range (Figure 1F). In specimens with a narrower coracoid base, which was not in direct continuation with the glenoid rim, the safe insertion range was much smaller (Figure 1E). This anatomic variation increased the standard deviation of the safe insertion range at this position (safe insertion range, 63.6° ± 17.6°). Despite the large average safe insertion angle, greater care should be taken in patients with a narrower base of the coracoid.

The Nevaiser portal[14] and the port of Wilmington[11] have been previously described for the treatment of SLAP lesions. Our simulated approach of the glenoid via these portals indicated that the port of Wilmington will permit a higher safe insertion range as compared with the approach via the Nevaiser portal. Moreover, the range at the 10:30 posterolateral position (simulating approach via port of Wilmington) was wider than the range at the 10:30 position. Therefore, if no other limitations exist, an oblique posterior approach to the glenoid rim at this location may provide surgeons with the maximal safe insertion range.[19]

At the 6:00 position, besides measuring the safe insertion range and optimal insertion angle, we wanted to study the direction that surgeons should use for successful anchor placement. We found that approaching the glenoid superior to the equator line always perforated the glenoid, while approaching the glenoid inferiorly to the equator line with either anterior or posterior angulation of the anchor permitted a safe anchor insertion. Lim et al[10] evaluated anchor penetration after Bankart repair in a cadaveric arthroscopic model. All anchors placed at 6:00 perforated the posteroinferior glenoid cortex. They related this observation to the deviation of anchor placement from the orthogonal position to the glenoid rim. Moreover, they found that these perforating anchors were biomechanically weaker relatively to anchors placed at 4:00.

Our study had the following limitations. First, we chose an anchor dimension (length 15 mm, width 3 mm) to represent a generic anchor size. Several other studies have used anchors with similar dimensions (14 × 3 mm in cadaveric anchor placement during glenoid labral repair).[6,10,13] Rapid changes in anchor technology have led to increased variability in anchor sizes, with the introduction of smaller anchors in width and length.[1] Smaller anchors may increase the margin for safety. Second, we placed our anchors at the edge of the glenoid rim along predefined directions; we did not take into account variations in vertical alignment. While we accounted for change in direction of the anchor to avoid the acromion, we did not account for changes in anchor placement to avoid the subscapularis tendon. Third, we did not collect information on donor hand dominance and activity (sports and work), which can influence glenoid anatomy. Fourth, this study does not account for the potential for the bone to undergo plastic deformation around the drill or the implant.

CONCLUSION

We placed virtual anchors at the edge of the glenoid rim along predefined directions. Optimal angles of insertion and maximum available range of deviation from the angle before perforation varied significantly with respect to the position on the glenoid face for placing labral fixation devices. The average optimal insertion angles we report can provide surgical guidelines to minimize the risk of perforation despite the subject-to-subject variation in glenoid morphology. Labral anchor insertion in the posterior glenoid rim typically required lower insertion angles and had a smaller margin of safety than did insertion in the anterior glenoid rim. To avoid the acromion while inserting an anchor at the 10:30 clockface position, a posterolateral oblique insertion was safer than an anterior oblique insertion angle. To place an anchor at the 6:00 position it is necessary to approach the glenoid from an inferior to superior direction to avoid perforation.

REFERENCES

1. Barber FA, Herbert MA. Cyclic loading biomechanical analysis of the pullout strengths of rotator cuff and glenoid anchors: 2013 update. *Arthroscopy*. 2013;29:832-844.
2. Chan H, Beaupre LA, Bouliane MJ. Injury of the suprascapular nerve during arthroscopic repair of superior labral tears: an anatomic study. *J Shoulder Elbow Surg*. 2010;19:709-715.
3. Chang EY, Fliszar E, Chung CB. Superior labrum anterior and posterior lesions and microinstability. *Magn Reson Imaging Clin N Am*. 2012; 20:277-294.
4. Davidson PA, Rivenburgh DW. The 7-o'clock posteroinferior portal for shoulder arthroscopy. *Am J Sports Med*. 2002;30:693-696.
5. Kaar TK, Schenck RC Jr, Wirth MA, Rockwood CA Jr. Complications of metallic suture anchors in shoulder surgery: a report of 8 cases. *Arthroscopy*. 2001;17:31-37.
6. Koh KH, Park WH, Lim TK, Yoo JC. Medial perforation of the glenoid neck following SLAP repair places the suprascapular nerve at risk: a cadaveric study. *J Shoulder Elbow Surg*. 2011;20:245-250.
7. Koulalis D, Kendoff D, Citak M, O'Loughlin PF, Pearle AD. Freehand versus navigated glenoid anchor positioning in anterior labral repair. *Knee Surg Sports Traumatol Arthrosc*. 2011;19:1554-1557.
8. Lehtinen JT, Tingart MJ, Apreleva M, Ticker JB, Warner JJ. Anatomy of the superior glenoid rim. Repair of superior labral anterior to posterior tears. *Am J Sports Med*. 2003;31:257-260.

9. Lehtinen JT, Tingart MJ, Apreleva M, Ticker JB, Warner JJ. Variations in glenoid rim anatomy: implications regarding anchor insertion. *Arthroscopy*. 2004;20:175-178.
10. Lim TK, Koh KH, Lee SH, et al. Inferior anchor cortical perforation with arthroscopic Bankart repair: a cadaveric study. *Arthroscopy*. 2013;29: 31-36.
11. Lo IK, Lind CC, Burkhart SS. Glenohumeral arthroscopy portals established using an outside-in technique: neurovascular anatomy at risk. *Arthroscopy*. 2004;20:596-602.
12. Mauro CS, Voos JE, Hammoud S, Altchek DW. Failed anterior shoulder stabilization. *J Shoulder Elbow Surg*. 2011;20:1340-1350.
13. Morgan R, Henn RF, Dreese JC. Anterosuperior portal injury to the suprascapular nerve during SLAP repair: a rotator interval portal is not safer than an anteroposterior portal. *Orthop J Sports Med*. 2013;1(4 suppl 1). doi:10.1177/2325967113S00046.
14. Nord KD, Masterson JP, Mauck BM. Superior labrum anterior posterior (SLAP) repair using the Neviaser portal. *Arthroscopy*. 2004; 20(suppl 2):129-133.
15. Park HB, Keyurapan E, Gill HS, Selhi HS, McFarland EG. Suture anchors and tacks for shoulder surgery, part II: the prevention and treatment of complications. *Am J Sports Med*. 2006;34:136-144.
16. Petrera M, Patella V, Patella S, Theodoropoulos J. A meta-analysis of open versus arthroscopic Bankart repair using suture anchors. *Knee Surg Sports Traumatol Arthrosc*. 2010;18:1742-1747.
17. Rhee YG, Lee DH, Chun IH, Bae SC. Glenohumeral arthropathy after arthroscopic anterior shoulder stabilization. *Arthroscopy*. 2004;20: 402-406.
18. Steinbach LS. MRI of glenohumeral instability. In: Chung CB, Steinbach LS, eds. *MRI of the Upper Extremity: Shoulder, Elbow, Wrist and Hand*. 1st ed. Philadelphia, PA: Lippincott Williams & Wilkins; 2009:280-282.
19. Yamamoto N, Itoi E, Abe H, et al. Effect of an anterior glenoid defect on anterior shoulder stability: a cadaveric study. *Am J Sports Med*. 2009;37:949-954.
20. Yoo JC, Lee YS, Ahn JH, Park JH, Kang HJ, Koh KH. Isolated suprascapular nerve injury below the spinoglenoid notch after SLAP repair. *J Shoulder Elbow Surg*. 2009;18:e27-e29.